ACS APPLIED MATERIALS & INTERFACES

www.acsami.org

Research Article

Micropatterned Biphasic Nanocomposite Platform for Maintaining Chondrocyte Morphology

Ram Saraswat, Ishara Ratnayake, E. Celeste Perez, William M. Schutz, Zhengtao Zhu, S. Phillip Ahrenkiel, and Scott T. Wood*

Cite This: *ACS Appl. Mater. Interfaces* 2020, 12, 14814−14824

Read Online

ACCESS | Metrics & More | Article Recommendations | Supporting Information

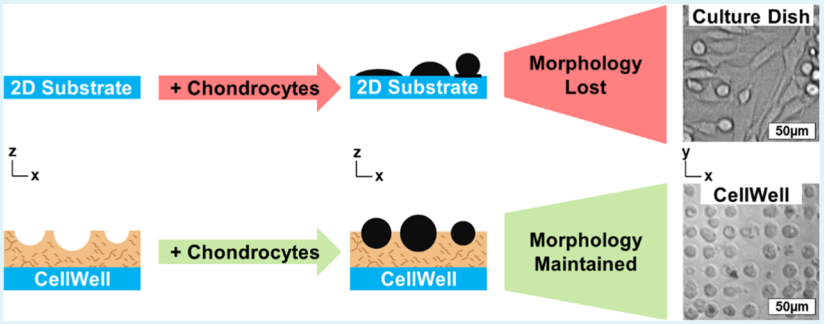

ABSTRACT: One major limitation hindering the translation of in vitro osteoarthritis research into clinical disease-modifying therapies is that chondrocytes rapidly spread and dedifferentiate under standard monolayer conditions. Current strategies to maintain rounded morphologies of chondrocytes in culture either unnaturally restrict adhesion and place chondrocytes in an excessively stiff mechanical environment or are impractical for use in many applications. To address the limitations of current techniques, we have developed a unique composite thin-film cell culture platform, the CellWell, to model articular cartilage that utilizes micropatterned hemispheroidal wells, precisely sized to fit individual cells (12−18 μm diameters), to promote physiologically spheroidal chondrocyte morphologies while maintaining compatibility with standard cell culture and analytical techniques. CellWells were constructed of 15-μm-thick 5% agarose films embedded with electrospun poly(vinyl alcohol) (PVA) nanofibers. Transmission electron microscope (TEM) images of PVA nanofibers revealed a mean diameter of 60.9 ± 24 nm, closely matching the observed 53.8 ± 29 nm mean diameter of human ankle collagen II fibers. Using AFM nanoindentation, CellWells were found to have compressive moduli of 158 ± 0.60 kPa at 15 μm/s indentation, closely matching published stiffness values of the native pericellular matrix. Primary human articular chondrocytes taken from ankle cartilage were seeded in CellWells and assessed at 24 h. Chondrocytes maintained their rounded morphology in CellWells (mean aspect ratio of 0.87 ± 0.1 vs three-dimensional (3D) control [0.86 ± 0.1]) more effectively than those seeded under standard conditions (0.65 ± 0.3), with average viability of >85%. The CellWell's design, with open, hemispheroidal wells in a thin film substrate of physiological stiffness, combines the practical advantages of two-dimensional (2D) culture systems with the physiological advantages of 3D systems. Through its ease of use and ability to maintain the physiological morphology of chondrocytes, we expect that the CellWell will enhance the clinical translatability of future studies conducted using this culture platform.

KEYWORDS: *articular cartilage model, micropatterned substrate, chondrocytes, morphology, hydrogel, nanofibers*

1. INTRODUCTION

Osteoarthritis (OA) is a painful disease of the articular joints that is primarily characterized by the degradation of the extracellular matrix (ECM) in the articular cartilage.[1] To date, surgical restoration techniques used for cartilage repair do not regenerate hyaline articular cartilage. Although symptoms can improve temporarily after surgical repair, 85% of patients progress to failure within 7.5 years or less.[2] There are currently no known medical treatments that effectively address the underlying molecular causes of OA. Current pharmaceutical treatment options are limited to the use of analgesics like nonsteroidal anti-inflammatory drugs (NSAID) and intra-articular corticosteroid injections to reduce the pain associated with inflammation, which only provides temporary relief and can have negative consequences with long-term use.[3−9] Articular chondrocytes are the only cells in the articular

Received: December 13, 2019
Accepted: March 12, 2020
Published: March 23, 2020

https://dx.doi.org/10.1021/acsami.9b22596
ACS Appl. Mater. Interfaces 2020, 12, 14814−14824

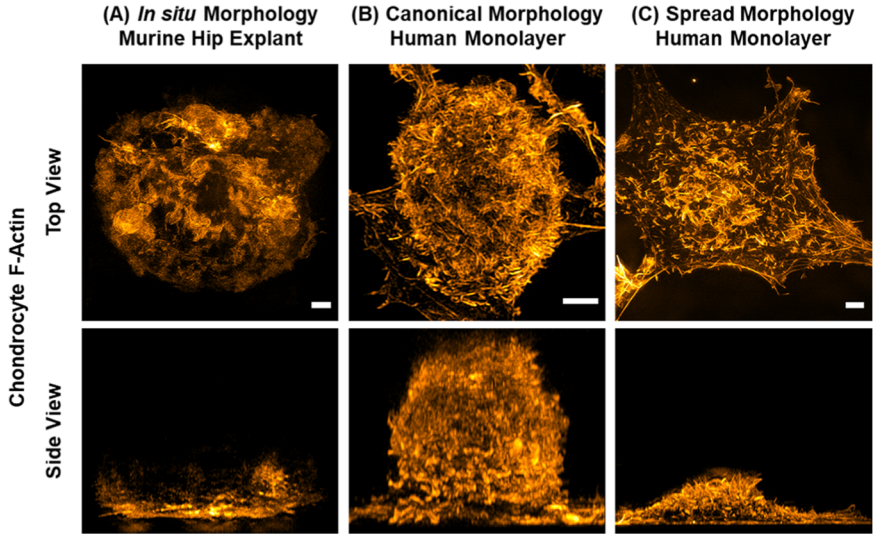

Figure 1. Chondrocyte morphology influences internal architecture. Murine femoral cap hip explants (A) and primary human articular chondrocytes (B) and (C) were plated on fibronectin (FN)-coated coverglass using standard 2D cell culture techniques, fixed with 4% paraformaldehyde, stained with ActinRed 555 Ready probes Reagent (ThermoFisher), and imaged in super-resolution using 3D structured illumination microscopy (3D-SIM) on a GE DeltaScan OMX SR microscope. Maximum intensity projections of volumetric image stacks are shown. Note in the side view of (A) that the turbidity of the tissue prevented imaging of all but the surface-most structures in the explant images, a common problem in imaging of both natural tissues and 3D cell cultures. Scale bars are 2 μm and apply to both top and side projections.

cartilage and are responsible for the maintenance of cartilage homeostasis between digestion and replacement of old or damaged tissue components. It is well accepted that a loss of this homeostatic balance is responsible for the development of OA.[10]

Animal models have long been the gold standard for understanding the progression of OA. However, they are also associated with concerns of ethical issues regarding the treatment of animals, cost and management issues, anatomical differences of cartilage in animals compared to humans, and age variations of animal species at the time of testing.[11−25]

Due to the problems associated with animal models, chondrocytes have been studied in vitro using either standard two-dimensional (2D) or any number of three-dimensional (3D) cell culture techniques. When plated on standard 2D platforms, chondrocytes tend to rapidly lose their canonical spheroidal morphology due to the adherent chondrocyte cells being on a hard and flat substrate and adopt a fibroblastic phenotype within 10−14 days of culture.[26−29] These morphological changes can result in substantial changes to chondrocyte architecture, including the length, density, and distribution of cortical actin fibers. The in situ chondrocyte shown in Figure 1A can be seen to have an actin network with length and density more similar to the chondrocyte displaying the canonical phenotype in Figure 1B than to that of the chondrocyte in Figure 1C, which has a spread morphology that is more typical of chondrocytes in standard monolayer culture (see Figure S1 for further details on actin fiber characterization). Note that the in situ chondrocyte in Figure 1A is not flat but that the turbidity of the tissue prevented imaging its full thickness, thereby illustrating the difficulties inherent to imaging cells in 3D samples. It has long been known that forcing chondrocytes to adopt a rounded morphology leads to enhancement of a chondrocyte phenotype in vitro; however, the techniques utilized previously have all relied upon restriction of binding area on a 2D substrate to prevent spreading rather than active promotion of a rounded phenotype in a way that does not inherently limit adhesion.[30,31]

In this study, we establish the proof-of-concept for a unique micropatterned nanocomposite cell culture platform, the CellWell, which consists of a thin film micropatterned nanofiber-embedded hydrogel substrate that fits a single cell within each well and facilitates high-throughput fluorescence imaging of chondrocytes. The substrate composition was chosen to recapitulate the ECM of articular cartilage wherein a hydrogel models cartilage proteoglycans and embedded nanofibers model collagen II fibers. Our goals for the design of the CellWell included (1) designing the wells such that their geometries reinforce the canonical spheroidal chondrocyte morphology for each cell, (2) matching the mechanical stiffness of articular cartilage ECM or the chondrocyte pericellular matrix (PCM) as closely as possible, (3) matching the diameters of the embedded nanofiber diameters as closely as possible to those of the native collagen II fibers, and (4) ensuring compatibility with traditional cell culture and live-cell imaging techniques.

2. MATERIALS AND METHODS

2.1. Materials Required. All of the reagents for hydrogels and fibers were purchased from Fisher Scientific unless otherwise noted. All of the reagents for transmission electron microscope (TEM) sample preparation were purchased from Ted Pella, Inc. (Redding, CA). Normal human articular cartilage samples from the ankle joint were obtained from the Thurston Arthritis Research Center (TARC) at the University of North Carolina (UNC) School of Medicine through the Department of Biochemistry at Rush University Medical Center (Chicago, IL), from the Gift of Hope Organ and Tissue Donor Network (Elmhurst, IL), and from Dakota Lions Sight and Health (Sioux Falls, SD).

2.2. Hydrogel Preparation. Agarose hydrogels (5% w/v) were prepared with slight modifications to the method described by Pauly et al.[32] Poly(vinyl alcohol) (PVA) (15% w/v) hydrogels were prepared based upon the method described by Jiang et al.[33]

2.3. Electrospun Nanofiber Preparation. PVA solution was prepared based upon the method described by Destaye et al.,[34] and

https://dx.doi.org/10.1021/acsami.9b22596
ACS Appl. Mater. Interfaces 2020, 12, 14814−14824

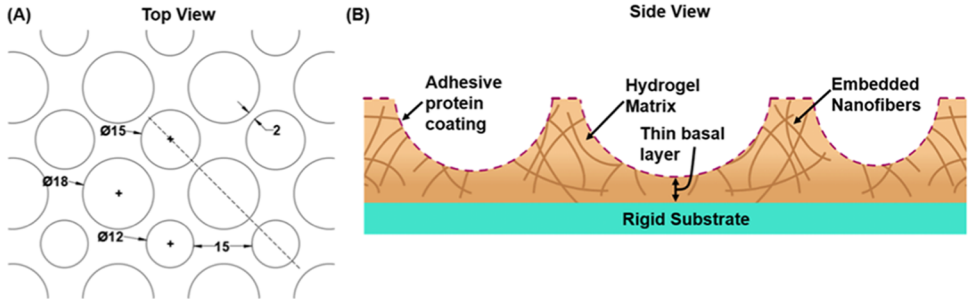

Figure 2. CellWell design schematics. (A) Representative section of photomask design. Units are in μm. (B) Cross-sectional representation of CellWell along the dashed line in (A).

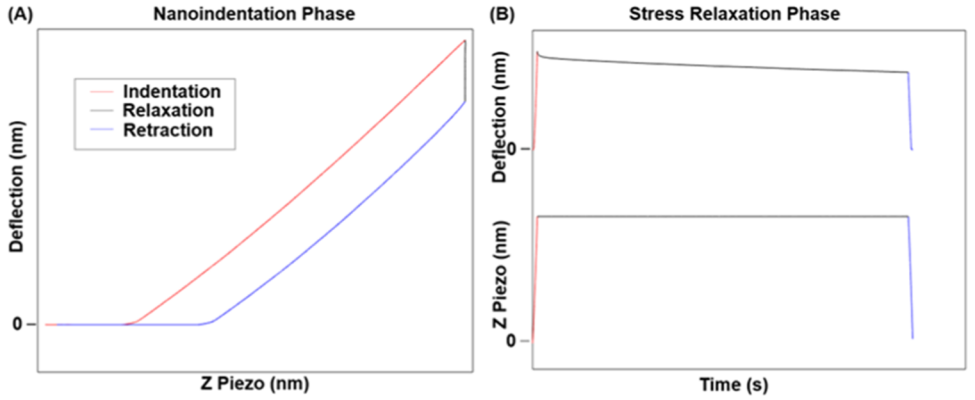

Figure 3. AFM experimental design schematics. (A) Nanoindentation phase. (B) Stress relaxation phase.

the electrospun nanofibers were obtained using the setup described by Mishra et al.[35] The electrospun nanofibers were then crosslinked under glutaraldehyde vapors for 48 h[34] in a vacuum desiccator.

2.4. CellWell Design and Manufacturing. The diameter of 8375 chondrocytes from 18 independent donors was measured using a Countless II FL cell counter (ThermoFisher). This information was used to establish the well diameters of the CellWell. Computer-aided design (CAD) files were generated in SolidWorks consisting of an array of circles of 12, 15, and 18 μm diameters and used to generate the photomask pattern, as shown in Figure 2. The design was chosen such that the distance between any two consecutive wells varied from 2 to 15 μm.

Micropatterned silicon wafers were obtained from the Utah Nanofab core lab at the University of Utah, and standard contact lithography techniques were utilized to generate PDMS CellWell stamps.[36] PDMS stamps were sterilized in an autoclave at 121 °C for 23 min.[37] "Containment chambers" were microfabricated with 15-μm-tall walls, in which the CellWell casting process took place. These walls were thus constructed to be ~8 μm taller than the hemispheroids in the stamps to provide room for several microns of material to separate the basal surface of the cells from the underlying coverglass without adding excessive bulk that can confound imaging experiments conducted on standard inverted microscopes. To cast CellWells, molten agarose solution, mixed with finely chopped crosslinked PVA nanofibers, was poured into a containment chamber, and the composite molten solution was stamped with a PDMS stamp at 4 °C for 6 min. The stamp was then removed, revealing the bare CellWell. CellWells were then immediately hydrated with PBS-1x solution, UV sterilized for 30 min, and coated with 10 μg/ml each of purified human plasma fibronectin and human placenta collagen type VI (Rockland Immunochemical) for 30 min at 37 °C. For polydopamine (PDA)-functionalized samples, agarose was coated with 2 mg/mL dopamine-HCl (10 mM Tris Buffer, pH 8.5, 24 h) at room temperature followed by coating with 25 μg/mL fibronectin for 24 h at 37 °C.

2.5. Cell Culture. Articular cartilage donors (N = 4) had an age range of 42–77, a male/female ratio of 2/2, Collins scores ranging from 0 to 2, and no known history of OA. Primary human articular chondrocyte isolation from deidentified ankle articular cartilage was performed as described previously.[38] Briefly, chondrocytes were isolated using sequential digestion with Pronase and collagenase, then plated in 35 mm tissue culture dishes and preincubated for 2 days to allow the cells to recover from the digestion process. Full-thickness articular cartilage explants were prepared before enzymatic digestion of the tissue using a 5 mm biopsy punch. Chondrocytes were gently lifted from the substrate using a 1 h treatment with Pronase and collagenase and then seeded onto CellWells or control substrates. Chondrocytes were plated on top of tissue culture polystyrene or 15-μm-thick nonpatterned agarose for 2D controls and encapsulated within thickness-matched agarose for 3D control samples.[39] In all cases, chondrocytes were seeded with a density of 2×10^5 cells/cm^2. Culture media was replaced at 1 h after initial seeding, after which cells were incubated continuously for 23 h before imaging on an Olympus IX71 inverted epifluorescence microscope with a 20×, 0.46 NA objective (Olympus) and an Andor iXon Ultra EMCCD camera (Andor). The viability of chondrocytes was assessed in CellWells at 24 h postseeding using a fluorescent ReadyProbes Cell Viability Imaging Kit (ThermoFisher).

2.6. Mechanical Characterization. The viscoelastic properties of CellWells and articular cartilage were analyzed using an Asylum Research MFP 3D atomic force microscope (AFM), with Igor Pro v6.37. Borosilicate glass spheres (4.8 ± 0.3 μm diameter; SPI Supplies) were attached to the tip of AFM cantilevers (force constant in the range 0.04–0.7 N/m; All-In-One-Al-Tipless, Budget Sensors) using epoxy, and spring constants for each cantilever were determined thermally[40,41] before experimentation. Stress relaxation of Agarose CellWells (N = 3) and articular cartilage explants (N = 3) was performed using a 5 μm/s approach velocity and 60 s relaxation time, as depicted in Figure 3. The indentation phase was utilized for all elastic parameter calculations, while the relaxation phase was utilized for all viscosity parameter calculations.

Once the raw curves were obtained, the raw deflection curves were converted to force curves using Hooke's Law

https://dx.doi.org/10.1021/acsami.9b22596
ACS Appl. Mater. Interfaces 2020, 12, 14814–14824

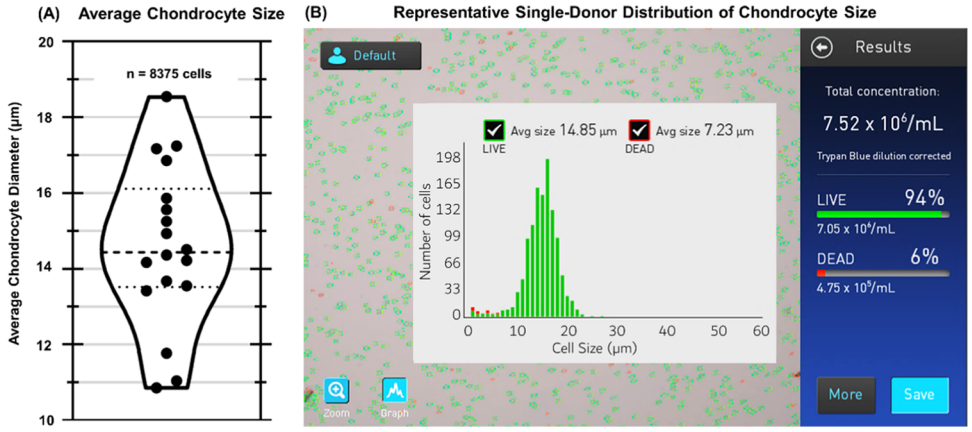

Figure 4. Chondrocyte diameter distribution. (A) Primary human articular chondrocytes were found to have a mean diameter of 14.6 ± 2.1 μm (SD) in suspension, with average diameters on a per-donor basis ranging from ∼11 to 19 μm. (B) Cell counter screenshot screen showing a representative single-donor chondrocyte diameter distribution.

$$F = kx \tag{1}$$

where F is the force, x is the deflection of the cantilever, and k is the cantilever spring constant determined thermally.

To analyze the viscoelastic properties, a modified version of the standard linear solid (SLS) model as described by Darling et al.[42] was used.

All of the force fittings were done as per the method described by Darling et al.,[42] described by the following equations

$$F = \frac{4E_Y}{3(1-\nu^2)} R^{1/2}\delta^{3/2} \tag{2}$$

$$F(t) = \frac{4E_Y}{3(1-\nu^2)} R^{1/2}\delta^{3/2}\left(1 + \frac{\tau_\sigma - \tau_\varepsilon}{\tau_\varepsilon} e^{-(t/\tau_\varepsilon)}\right) \tag{3}$$

$$k_1 = E_R \tag{4}$$

$$k_2 = E_R \frac{(\tau_\sigma - \tau_\varepsilon)}{\tau_\varepsilon} \tag{5}$$

$$\mu = E_R(\tau_\sigma - \tau_\varepsilon) \tag{6}$$

$$E_0 = E_R\left(1 + \frac{\tau_\sigma - \tau_\varepsilon}{\tau_\varepsilon}\right) \tag{7}$$

$$E_Y = 1.5E_R \tag{8}$$

where E_Y is the Hertz Compressive Moduli, F is the applied force during indentation, ν is the Poisson's ratio, R is the radius of the indenter (2.5 μm), $F(t)$ is the force measured as a function of time during stress relaxation, E_R is the SLS Relaxation Moduli, τ_σ is the relaxation time under constant load, τ_ϵ is the relaxation time under constant deformation, k_1 and k_2 are the Kelvin spring elements, μ is the apparent viscosity, and E_0 is the instantaneous moduli.

As per Darling et al.,[42] eq 2 fits the Hertz equation, and eq 3 fits the standard linear solid (SLS) model. The Poisson's ratio of agarose and cartilage were both assumed to be 0.33,[43] and calculations were performed based on measurements at 1,500 nm of indentation depth (10% compressive strain for CellWells).

Agarose CellWells (N = 3) were separately indented at 15 μm/s to allow for direct comparison of compressive moduli with that of human pericellular matrix published by Darling et al.[44] For this comparison, the compressive moduli were obtained using eq 2 at 8% compressive strain. All of the mechanical measurements were taken between the wells due to the curvature of the wells limiting the ability to take AFM measurements within wells. To assess the stiffness within wells, the modulus of agarose samples with a thickness corresponding to the thickness of the CellWell at the bottom of wells (7 μm) was measured. Agarose samples of 3 μm thickness were also assessed to confirm a lack of substrate effects.

2.7. Optical Transmittance. Optical transmittance of agarose, PVA nanofibers, and nanofiber-embedded CellWells (N = 3 each) in the visible range was measured using a video spectral comparator (VSC). Transmittance values were normalized against coverglass controls.

2.8. Nanofiber Characterization. PVA and ankle cartilage collagen II nanofibers were imaged using a JEOL JEM-2100 LaB_6 transmission electron microscope (TEM), and diameters were measured using FIJI ImageJ v1.52n. PVA nanofibers were prepared as described in 2.3 and mounted on TEM grids for imaging. For collagen II diameter measurements, articular cartilage explants from the ankle were fixed with 2% PFA and 2.5% glutaraldehyde in 0.1 M cacodylate solution for 1 h, followed by rinsing with sodium cacodylate buffer (0.1 M, pH 7.2) three times for 5 min each. Then, the tissues were postfixed with 0.5% OsO_4 and 0.5% potassium ferrocyanide for 30 min. After rinsing with cacodylate buffer, the tissues were dehydrated in a series of ethanol solutions (50, 70, 90, and 100% for 20 min each). The tissues were infiltrated with a mixture of ethanol and Araldite (2:1, 1:1, 1:2 ratios for 2 h each) and cured with a fresh Araldite resin at 60 °C for 48 h. Sections of 70 nm thickness were cut with an ultramicrotome (RMC Powertome XL), mounted on TEM grids, and stained with uranyl acetate and lead citrate.

2.9. Statistical Analysis. Data from a minimum of three independent experiments were analyzed for all statistical analyses. Linear regression was used to determine the quality of fit of Hertzian and viscoelastic models to AFM indentation data. Cell morphology measurements were collected on a single-cell basis. A Shapiro–Wilk test was used to determine whether data sets had normal or lognormal distributions. A Kruskal–Wallis test with Dunn's multiple comparison post hoc test was used to determine effects since data sets were found to have neither normal nor lognormal distributions. All statistical analyses were performed in GraphPad Prism v8.2.1.

3. RESULTS

3.1. Chondrocyte Diameter. As shown in Figure 4A, human chondrocytes were found to have a mean diameter of 14.6 μm ± 2.1 μm (standard deviation, SD), and this data represented the diameter measurements from 8,375 cells over n = 18 individual donors. For each donor, the cell counter provided direct measurements of cell density (i.e., number), viability (based on trypan blue exclusion, circularity, and diameter), and average diameter, as well as a pictographic histogram of the distribution of diameters within the sample. The chondrocyte diameter distribution of average donors

https://dx.doi.org/10.1021/acsami.9b22596
ACS Appl. Mater. Interfaces 2020, 12, 14814−14824

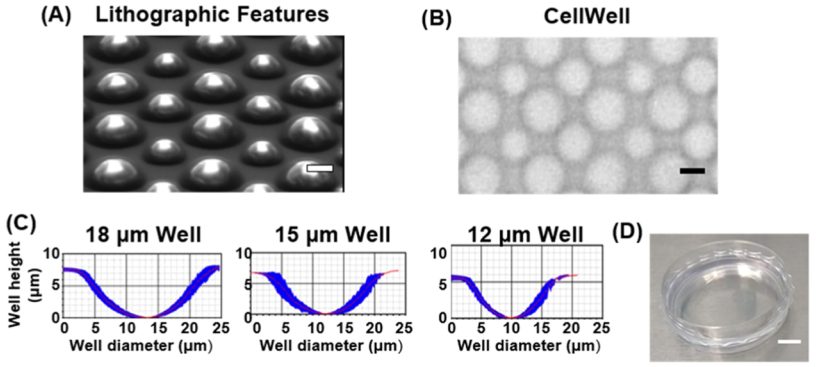

Figure 5. Micropatterned wells match chondrocyte diameters. (A) Scanning electron microscopy (SEM) image of lithographic patterns used to create CellWells. (B) Phase-contrast image of CellWell with three sizes of wells precisely sized to fit individual articular chondrocytes; scale bars 10 μm. (C) Optical profilometry cross-sectional profiles of individual wells (mean ± SD of n = 10 wells each). (D) Macroappearance of the CellWell; scale bar 5 mm.

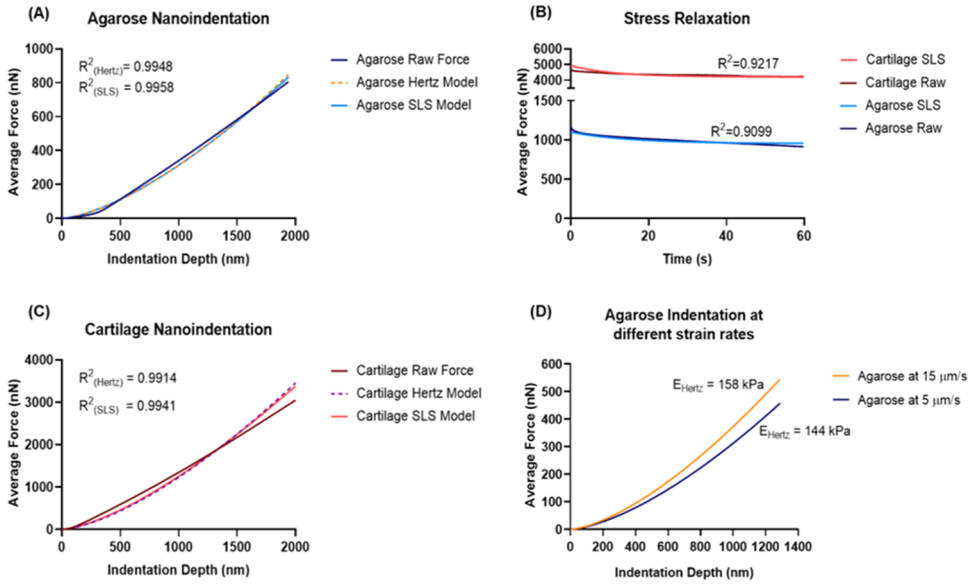

Figure 6. Mechanical characterization of CellWell agarose and ankle articular cartilage. (A) Average nanoindentation curves of agarose CellWells. (B) Average stress relaxation of agarose CellWells and articular cartilage. (C) Average nanoindentation curves of articular cartilage. (D) Average nanoindentation on agarose CellWells at different strain rates.

depicted a full width at half maxima (FWHM) of 12−18 μm, as shown in Figure 4B. These measurements served as the basis for the selection of CellWell diameters of 12, 15, and 18 μm.

3.2. CellWell Manufacturing. A Keyence VK-X250 optical profilometer was used to measure the dimensions of CellWell features (N = 10). One of the limitations of our profilometer was that it could only work with dry samples and so we expected shrinkage effects in our CellWells due to the fact that the gelation mechanism of agarose is solely based on the physical hydrogen-bond networks.[45−48] Thus, to ensure the fidelity of collected data, CellWells for these measurements were made out of PVA because PVA was made by the freeze−thaw method as described in Section 2.2, and frozen samples were able to be utilized to minimize the loss of feature height due to hydrogel drying compared to CellWells made of agarose. Figure 5A shows scanning electron microscopy (SEM) images of the lithographic patterns on silicon that were used to create CellWell stamps. Figure 5B shows a phase-contrast image of a CellWell with three sizes of wells precisely sized to fit individual articular chondrocytes. Figure 5C shows the cross-sectional profiles of individual wells as measured by optical profilometry. Although frozen PVA CellWells were observed to have a decrease in well height by 7−15% due to imaging in the dried state, it can be easily seen in Figure 5C that the geometry of the wells is hemispheroidal. The macroappearance of the CellWell is shown in Figure 5D.

3.3. Mechanical Characterization. Figure 6A,C depicts average indentation curves at 5 μm/s for agarose and cartilage (N = 3), respectively, along with both Hertzian (eq 2) and viscoelastic SLS model (eq 3) fits. Figure 6B depicts average stress relaxation curves for agarose and cartilage along with the respective SLS fit for each based on eq 3. These models were used to analyze the mechanical properties of agarose CellWells and ankle articular cartilage, as shown in Table 1.

Figure 6 and Table 1 show comparisons of the CellWell with human ankle articular cartilage. While slightly less stiff than cartilage as measured by AFM, the CellWell provides a much more comparable mechanical environment to the articular cartilage (70% lower) than commonly used tissue culture polystyrene (10^4 higher), coverglass (10^5 higher), or softer hydrogels (10^2 lower). Thus, the CellWell provides a much

https://dx.doi.org/10.1021/acsami.9b22596
ACS Appl. Mater. Interfaces 2020, 12, 14814−14824

Table 1. Comparison of Mechanical Properties of the Agarose CellWells and Articular Cartilage[a]

mechanical parameter	CellWell	articular cartilage
Hertz elastic modulus, E_Y (kPa)	144 ± 11.5	488 ± 102.5
relaxation modulus, E_R (kPa)	95.8 ± 7.65	325 ± 68.3
instantaneous modulus, E_0 (kPa)	175 ± 24.5	575 ± 126.5
τ_σ (s)	17.3 ± 1.04	15.0 ± 4.80
τ_ϵ (s)	14.3 ± 0.86	12.8 ± 4.09
k_1 (kPa)	95.8 ± 7.65	325 ± 68.3
k_2 (kPa)	20.8 ± 7.90	58.0 ± 16.8
μ (kPa·s)	296 ± 103.6	677 ± 60.9

[a]Mean ± SD.

more appropriate mechanical environment for the cells than standard monolayer cultures.

To compare the compressive mechanical properties of CellWells with that of human extracellular and pericellular matrices published by Darling et al.,[44] we indented the agarose CellWells at 15 μm/s. As a comparison, the agarose at 5 μm/s was also plotted to depict the effect of strain rate, as shown in Figure 6D. Importantly, the CellWell elastic modulus of 158 ± 0.6 kPa (SD) at 15 μm/s strain rate is very close to the reported, strain-rate matched, 162 ± 22 kPa (SD) stiffness of knee cartilage PCM, indicating that it provides a highly appropriate mechanical environment for chondrocytes. As shown in Table S1, no substantial difference was observed between the stiffness of CellWells and agarose films of 7 and 3 μm stiffness, suggesting that the stiffness of the CellWell is homogeneous within and between wells and that the thickness of the CellWell is sufficient to avoid substrate effects on the stiffness.

3.4. Optical Characterization. In general, the turbidity of 3D samples makes it difficult to image them beyond their surface level. To ensure that the CellWells are optically transparent enough to facilitate clear imaging on an inverted microscope with standard live-cell imaging techniques, we measured the optical transmittance of the CellWells across the visible range (Figure 7). Even though the nanofibers had a

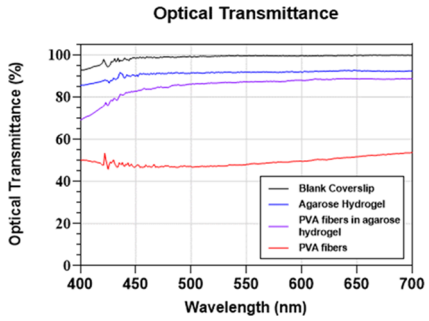

Figure 7. Optical transmittance of the CellWells measured using Video Spectral Comparator, confirming the optical transparency of the CellWells.

transmittance of only about 50%, the transmittance of the hydrogels was found to be higher than 85%, and the nanofiber-embedded hydrogels ranged from 70 to 85%.

3.5. Protein Coating. To confirm the adsorption of PCM proteins onto agarose CellWells, Fourier transform infrared spectra (FTIR) of coated CellWells were obtained for samples coated with either fibronectin (FN) or type-VI collagen (Col-VI). The FTIR spectra of an uncoated agarose CellWell and pure PCM proteins were also analyzed and used as controls. As depicted in Figure 8, the FTIR spectra of agarose CellWells

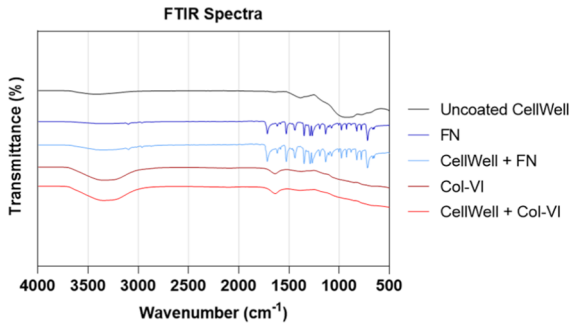

Figure 8. Successful coating of PCM proteins on the CellWells as confirmed by FTIR spectroscopy.

coated with FN or Col-VI were representative of the pure proteins, thus confirming that the PCM proteins were successfully adsorbed onto CellWells. However, a major limitation of this strategy is that the proteins do not adsorb strongly to agarose, which both limits initial cell adhesion and leads to a drastic loss of cell adhesion beyond 24−36 h after seeding.

3.6. Nanofiber Characterization. Since the nanofibers were embedded into the Agarose CellWells to model collagen II fibers within articular cartilage, it was essential to obtain the distribution of their diameters. To the authors' knowledge, the diameters of collagen II nanofibers in ankle cartilage have never been reported; thus, their measurement was necessary here to optimize the conditions for electrospinning CellWell PVA nanofibers. Figure 9A,B shows representative TEM

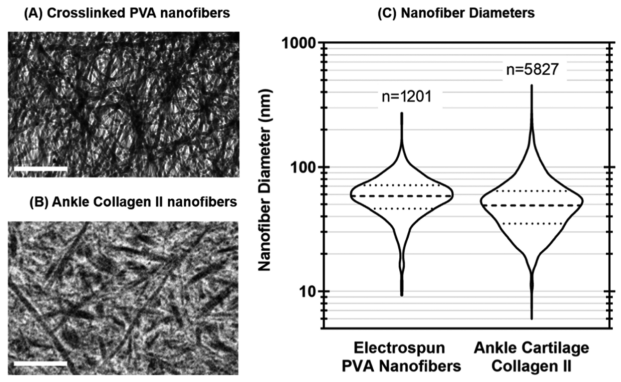

Figure 9. Electrospun PVA nanofibers have a diameter distribution representative of collagen II fibers in ankle articular cartilage. TEM images of (A) PVA nanofibers post-crosslinking and (B) collagen II fibers, extracted from the ankle; scale bars 1 μm. (C) Distribution of crosslinked PVA nanofibers to recapitulate the nature of the collagen II fibers of the extracellular matrix of articular cartilage within our CellWell articular cartilage model for isolated chondrocyte cell culture. Fiber measurements were obtained from n = 3 independent samples, with individual measurements represented on the graph.

images of both crosslinked PVA nanofibers and ankle articular cartilage, respectively. As seen in Figure 9C, the collagen II nanofibers had a median diameter of 50 nm compared to the 60 nm median diameter of PVA nanofibers. The PVA nanofibers were found to be within 10 nm for the median as well as the 25th and 75th quartiles of the ankle collagen II

https://dx.doi.org/10.1021/acsami.9b22596
ACS Appl. Mater. Interfaces 2020, 12, 14814−14824

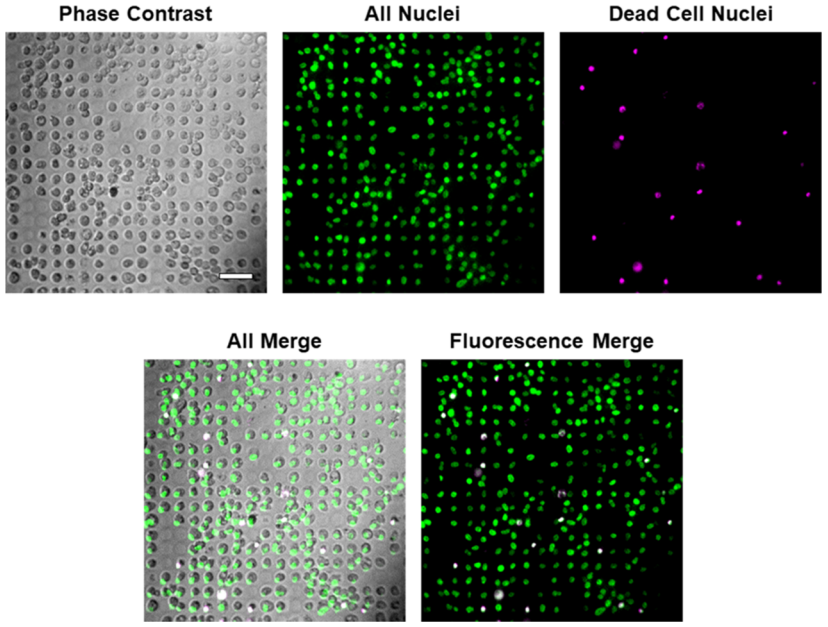

Figure 10. Chondrocyte viability is maintained in the CellWell. Chondrocyte viability of 85.6 ± 10.5% (SD) was observed at 24 h using a standard inverted epifluorescence microscope. Cell-permeable NucBlue stains all nuclei (shown in green), while cell-impermeable NucGreen stains only the nuclei of (dead) cells whose membranes have been disrupted (shown in magenta; dead cells appear white in overlaid images). Scale bar 50 μm.

nanofibers as well, substantiating the use of PVA nanofibers to model the collagen II nanofibers in the CellWell.

3.7. Chondrocyte Viability. A fluorescent viability assay (ReadyProbes Cell Viability Imaging Kit, ThermoFisher) was conducted to assess both the cytotoxicity of the CellWell and its compatibility for use with standard live-cell imaging techniques, as shown in Figure 10. At 24 h postseeding, viability of 85.6 ± 10.5% (SD) was observed.

3.8. Chondrocyte Morphology. As depicted in Figure 11, we have found that the CellWell is highly effective at promoting a physiological rounded chondrocyte morphology at 24 h of culture, as measured against standard 2D culture and 3D culture controls in which chondrocytes were embedded within agarose. Figure 11 shows phase-contrast images and aspect ratios of chondrocytes seeded in agarose CellWells and control substrates—atop tissue culture polystyrene or agarose (2D culture) or encapsulated within agarose (3D culture). It can be easily seen that within 24 h postseeding, many chondrocytes in 2D culture had lost their canonical spheroid morphology and started to spread. On the other hand, the chondrocytes in CellWells maintained their canonical morphology similar to those in 3D agarose culture. No statistical difference was observed between 3D agarose and CellWell chondrocyte morphologies, indicating maintenance of physiological morphology by the CellWell, while all other samples were found to be significantly different from each other. To assess the height of cells in wells, cross-sectional measurements of the chondrocyte area on each substrate were obtained. As shown in Figure S2, the area of the cells in CellWells closely matched the area of the cells in 3D encapsulated agarose, both of which were significantly lower, and therefore presumably taller, than the more spread cells plated on 2D controls.

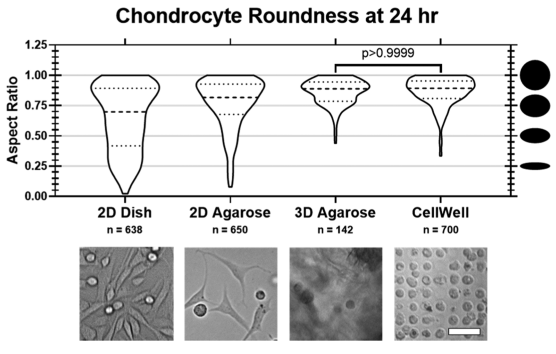

Figure 11. CellWells promote maintenance of physiological chondrocyte morphology. (A) Phase-contrast images of chondrocytes seeded using various platforms at 24 h are shown below distributions of aspect ratios of chondrocytes seeded with each platform from $n = 3$ donors. No difference was observed between 3D agarose and CellWell chondrocyte morphologies, indicating CellWell maintenance of physiological morphology, while all other samples were significantly different from each other ($p \leq 0.0002$) based on Kruskal–Wallis with Dunn's multiple comparison post hoc test. Scale bar 50 μm.

3.9. Long-Term Chondrocyte Morphology Maintenance. To achieve a long-term adherent culture, strong surface chemistry is required to bind the PCM proteins onto the hydrogel surface. We found that a polydopamine (PDA)-based strategy can successfully maintain chondrocyte adherence for long-term culture up to 28 days, as shown in Figure 12. This is a novel strategy that, to our knowledge, has never been used to modify the surface of agarose hydrogels.

4. DISCUSSION

We have presented here a unique micropatterned nanocomposite cell culture platform to model articular cartilage that is suitable for high-throughput single-cell analyses of live cells using standard imaging techniques. All of the images in Figures 10 and 11 were obtained using a standard inverted epifluorescence microscope. Contrary to some 2D micropatterned approaches,[49] we do not have any nonadhesive areas to promote the cells being in a pattern. The geometry and

https://dx.doi.org/10.1021/acsami.9b22596
ACS Appl. Mater. Interfaces 2020, 12, 14814−14824

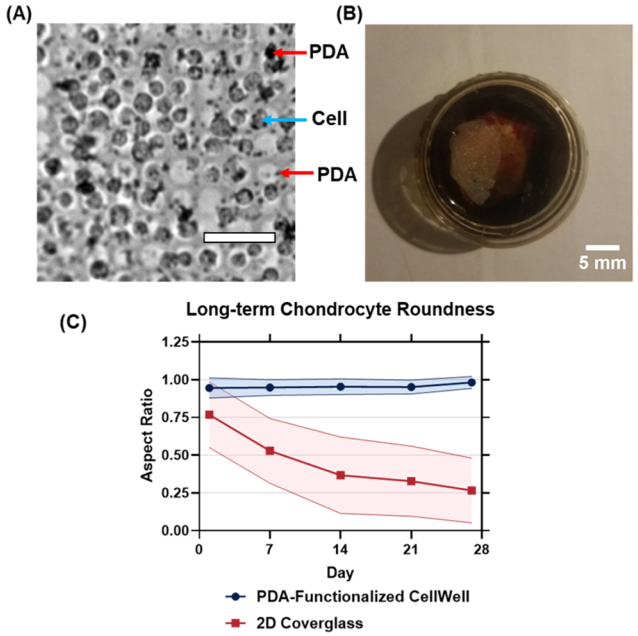

Figure 12. Polydopamine functionalization promotes chondrocyte morphology maintenance in the CellWell for a 28-day period. (A) Phase-contrast image of chondrocytes seeded for 4 weeks in a CellWell show robust maintenance of canonical spheroidal morphology; Blue arrow: chondrocyte; Red arrows: large and small particles of PDA aggregation; Scale Bar 50 μm. (B) Macroscopic appearance of PDA-functionalized CellWell shows a substantial darkening of the agarose. (C) Aspect ratio measurements (mean ± SD, n = 150 cells) over a period of 4 weeks show strong long-term maintenance of spheroidal morphology by the CellWell (p < 0.0001 relative to 2D coverglass at each time point based on Kruskal–Wallis test with Dunn's multiple comparison post hoc analysis).

spacing of our wells naturally promote the chondrocytes to fall into the wells.

Two-dimensional substrates coated with nonadhesive polymers (e.g., poly(ethylene glycol) [PEG] or poly[2-hydroxyethyl methacrylate] [poly(HEMA)]), 2D substrates micropatterned with small circular islands of ECM proteins or amine groups surrounded by nonadhesive polymers, and suspension culture have all been shown to promote maintenance of a rounded morphology and expression of phenotypic markers in chondrocytes.[30,50,51] However, their 50 μm^2 contact area is only 4.9–11% of the surface area of a typical articular chondrocyte (Figure 4). This lack of adhesion can have unintended and unpredictable consequences on cell signaling behavior—especially in studies of integrin-mediated mechanotransduction, which is well known to be an essential mechanism of mechanotransduction in many cell types (although it has not been extensively examined in articular chondrocytes). By contrast, the CellWell design should provide a contact area (226–509 μm^2, depending on well diameter) of approximately 50% of the surface area of each cell seated directly within a well. Furthermore, the previous 2D micropatterning technique relies on culturing cells directly on a coverslip, which adversely affects the mechanical environment of the chondrocytes, since the coverglass stiffness is ~10^5 Pa higher than that of the articular cartilage overall and ~10^6 Pa higher than that of the chondrocyte PCM.

3D culture platforms (e.g., multicellular spheroids, organoids, and scaffolds)[52] have also been shown to promote maintenance of chondrocyte phenotype;[51,53–60] however, these techniques severely restrict the number of compatible analytical techniques, especially those capable of observing sensitive post-translational modifications of proteins that are key to cell signaling pathways. Moreover, 3D cultures are inherently difficult to image cells within, with high-quality images typically only attainable along the surface of samples (as in Figure 1A).

To combine the advantages of 2D and 3D cell culture techniques, we have presented a unique micropatterned nanocomposite cell culture platform, the CellWell. The CellWell models the ECM of articular cartilage by utilizing a substrate composed of a hydrogel (to model cartilage proteoglycans) embedded with nanofibers (to model cartilage collagen II nanofibers). It is further micropatterned with a network of wells that are designed with geometries intended to reinforce the canonical spheroidal chondrocyte morphology. The CellWell addresses the problems of previous micropatterning techniques by providing a micropatterned environment that is much closer to the stiffness of the PCM than coverglass or tissue culture plastic and can promote adhesion.

One recent study utilized a similar philosophical approach to the CellWell by using ion milling of agarose to generate "cell hotels" for individual *E. coli* cells.[61] However, the agarose used in that study had a thickness of ~1 mm, which precluded its use for live-cell imaging. By utilizing a thin basal layer of only ~8 μm between the well bottoms and the underlying rigid substrate (e.g., coverglass or tissue culture dish), the CellWell provides a unique system that nestles only one cell per well, thus facilitating high-throughput single-cell analysis of live cells with standard imaging techniques.

Another advantage of the CellWell over previous micropatterning techniques is the relatively minimal distance between wells. Instead of utilizing a large fixed distance of 30 μm or greater between any two consecutive wells,[31,44] the CellWell provides a range of distances between consecutive wells ranging from a minimal distance of 2.5 μm (slightly larger than the separation between cell pairs within chondrons in vivo) to a maximum distance of 15 μm. This, in combination with the fact that the wells are only approximately half the height of the cells, provides cells with the flexibility to either directly contact their neighboring cells by reaching over the space between wells or to remain in isolation. This flexibility provides immense possibilities for researchers interested in understanding the effects of cell–cell contact mechanics. Another advantage of the CellWell is the variable well diameters. Chondrocytes, like most cells, have a wide range of sizes. By providing a platform with a representative distribution of well diameters, the CellWell can provide a more natural environment for any given cell than systems with single fixed diameters.

In the current study, we have provided proof-of-principle for the CellWell as an articular cartilage model to prevent dedifferentiation of articular chondrocytes that also facilitates high-throughput live-cell imaging studies. We found that a PDA-based surface functionalization strategy can enable the CellWell to successfully maintain chondrocyte adherence for long-term cultures. Only two previous studies have used PDA chemistry to functionalize biomaterials for the culture of articular chondrocytes, neither of which utilized human cells or agarose.[62,63]

The CellWell is a micropatterned substrate that we have shown is capable of successfully maintaining the canonical spheroidal morphology over a period of 28 days. Previous

https://dx.doi.org/10.1021/acsami.9b22596
ACS Appl. Mater. Interfaces 2020, 12, 14814–14824

micropatterning-based techniques designed to maintain the morphology of human chondrocytes have only been shown to be successful for a maximum of 7 days.[31,51] However, a limitation of the current PDA-based functionalization strategy is the darkness of the polydopamine layer due to the concentration of PDA used (Figures 12B and S3). For this initial study, 2 mg/mL PDA was utilized, as this is the most common concentration used across the literature.[64−66] In future studies, we will seek to optimize the PDA concentration to balance surface chemistry with optical transparency, thereby enabling us to validate the phenotypic expression of phenotype marker proteins using immunofluorescence. We will also endeavor to develop a second-generation CellWell with multiple well geometries to model different depth zones of the articular cartilage.

5. CONCLUSIONS

We have demonstrated our ability to successfully synthesize a novel biphasic micropatterned platform—the CellWell. The compressive modulus of the CellWell was very close to that previously reported for the pericellular matrix of knee cartilage.[44] Ankle collagen II nanofiber diameters have been reported for the first time, and our crosslinked electrospun PVA nanofibers were found to have a diameter distribution representative of collagen II fibers. The micropatterned hemispheroidal wells in the CellWell promoted the canonical spheroidal morphology of articular chondrocytes with reasonable cell viability observed. Single-cell imaging was easily performed using a standard 20× objective on an inverted epifluorescence microscope due to the optical translucency of the CellWell (essentially a micropatterned thin film), and the embedded nanofibers were not found to inhibit optical translucency. These findings substantiate the applicability of the CellWell for use with standard culture and single-cell analysis techniques for live-cell imaging. The CellWell also has the advantage of material flexibility, with synthesis demonstrated using multiple hydrogel materials (i.e., agarose and PVA). Ultimately, we expect that by maintaining the physiological morphology of chondrocytes, the CellWell will promote the physiological arrangement of intracellular structural proteins, thereby enhancing the clinical translatability of future studies conducted using this culture platform.

■ ASSOCIATED CONTENT

Supporting Information

The Supporting Information is available free of charge at https://pubs.acs.org/doi/10.1021/acsami.9b22596.

Quantitative analysis of actin fibers from in situ chondrocytes in a murine hip explant (mouse) (Figure S1); distribution of chondrocyte *XY* area on the different platforms from n = 3 donors (Figure S2); compressive stiffness of agarose at different thicknesses (Table S1) (PDF)

■ AUTHOR INFORMATION

Corresponding Author

Scott T. Wood − *Nanoscience and Nanoengineering, South Dakota School of Mines & Technology, Rapid City, South Dakota 57701, United States;* orcid.org/0000-0002-6747-0547; Phone: +1-605-394-5222; Email: scott.wood@sdsmt.edu

Authors

Ram Saraswat − *Nanoscience and Nanoengineering, South Dakota School of Mines & Technology, Rapid City, South Dakota 57701, United States*

Ishara Ratnayake − *Nanoscience and Nanoengineering, South Dakota School of Mines & Technology, Rapid City, South Dakota 57701, United States*

E. Celeste Perez − *Nanoscience and Nanoengineering, South Dakota School of Mines & Technology, Rapid City, South Dakota 57701, United States*

William M. Schutz − *Nanoscience and Nanoengineering, South Dakota School of Mines & Technology, Rapid City, South Dakota 57701, United States*

Zhengtao Zhu − *Nanoscience and Nanoengineering and Chemistry and Applied Biological Sciences, South Dakota School of Mines & Technology, Rapid City, South Dakota 57701, United States;* orcid.org/0000-0002-9311-2110

S. Phillip Ahrenkiel − *Nanoscience and Nanoengineering, South Dakota School of Mines & Technology, Rapid City, South Dakota 57701, United States*

Complete contact information is available at: https://pubs.acs.org/10.1021/acsami.9b22596

Author Contributions

S.T.W. conceived of the presented idea and supervised the project. R.S., I.R., E.C.P., and W.M.S. carried out and analyzed the experiments. Z.Z. and S.P.A. contributed to lithography and electrospinning experimental design, respectively. R.S. wrote the manuscript with support from I.R. and S.T.W. All authors provided critical feedback and helped shape the research, analysis, and manuscript.

Notes

The authors declare no competing financial interest.

■ ACKNOWLEDGMENTS

We thank Dakota Lions Sight and Health, the Gift of Hope Tissue and Organ Donor Network, Dr. Susan Chubinskaya, Dr. Richard Loeser, and donor families for providing normal donor tissue. We thank Brian Baker at Utah Nanofab for his technical assistance in providing the micropatterned silicon wafers. This material is based upon work supported by the National Science Foundation/EPSCoR Cooperative Agreement #IIA-1355423 and by the State of South Dakota. Any opinions, findings, and conclusions or recommendations expressed in this material are those of the author(s) and do not necessarily reflect the views of the National Science Foundation.

■ REFERENCES

(1) Lawrence, R. C.; Felson, D. T.; Helmick, C. G.; Arnold, L. M.; Choi, H.; Deyo, R. A.; Gabriel, S.; Hirsch, R.; Hochberg, M. C.; Hunder, G. G.; Jordan, J. M.; Katz, J. N.; Kremers, H. M.; Wolfe, F. Estimates of the prevalence of arthritis and other rheumatic conditions in the United States. Part II. *Arthritis Rheum.* **2008**, *58*, 26−35.

(2) DiBartola, A. C.; Everhart, J. S.; Magnussen, R. A.; Carey, J. L.; Brophy, R. H.; Schmitt, L. C.; Flanigan, D. C. Correlation between histological outcome and surgical cartilage repair technique in the knee: A meta-analysis. *Knee* **2016**, *23*, 344−349.

(3) Kavanaugh, T. E.; Werfel, T. A.; Cho, H.; Hasty, K. A.; Duvall, C. L. Particle-based technologies for osteoarthritis detection and therapy. *Drug Delivery Transl. Res.* **2016**, *6*, 132−147.

(4) Lee, A. S.; Ellman, M. B.; Yan, D.; Kroin, J. S.; Cole, B. J.; van Wijnen, A. J.; Im, H. J. A current review of molecular mechanisms regarding osteoarthritis and pain. *Gene* **2013**, *527*, 440−447.
(5) Bijlsma, J. W.; Berenbaum, F.; Lafeber, F. P. Osteoarthritis: an update with relevance for clinical practice. *Lancet* **2011**, *377*, 2115−2126.
(6) Bradley, J. D.; Brandt, K. D.; Katz, B. P.; Kalasinski, L. A.; Ryan, S. I. Comparison of an antiinflammatory dose of ibuprofen, an analgesic dose of ibuprofen, and acetaminophen in the treatment of patients with osteoarthritis of the knee. *N. Engl. J. Med.* **1991**, *325*, 87−91.
(7) Kirwan, J. R. The effect of glucocorticoids on joint destruction in rheumatoid arthritis. The Arthritis and Rheumatism Council Low-Dose Glucocorticoid Study Group. *N. Engl. J. Med.* **1995**, *333*, 142−146.
(8) Kirwan, J. R.; Rankin, E. Intra-articular therapy in osteoarthritis. *Bailliere's Clin. Rheumatol.* **1997**, *11*, 769−794.
(9) Derendorf, H.; Mollmann, H.; Gruner, A.; Haack, D.; Gyselby, G. Pharmacokinetics and pharmacodynamics of glucocorticoid suspensions after intra-articular administration. *Clin. Pharmacol. Ther.* **1986**, *39*, 313−317.
(10) Andriacchi, T. P.; Mundermann, A.; Smith, R. L.; Alexander, E. J.; Dyrby, C. O.; Koo, S. A framework for the in vivo pathomechanics of osteoarthritis at the knee. *Ann. Biomed. Eng.* **2004**, *32*, 447−457.
(11) Cope, P. J.; Ourradi, K.; Li, Y.; Sharif, M. Models of osteoarthritis: the good, the bad and the promising. *Osteoarthritis Cartilage* **2019**, *27*, 230−239.
(12) Bendele, A. M. Animal models of osteoarthritis. *J. Musculoskeletal Neuronal Interact.* **2001**, *1*, 363−376.
(13) Bendele, A. M.; Hulman, J. F. Effects of body weight restriction on the development and progression of spontaneous osteoarthritis in guinea pigs. *Arthritis Rheum.* **1991**, *34*, 1180−1184.
(14) Silberberg, M.; Silberberg, R. Age changes of bones and joints in various strains of mice. *Am. J. Anat.* **1941**, *68*, 69−95.
(15) Gregory, M. H.; Capito, N.; Kuroki, K.; Stoker, A. M.; Cook, J. L.; Sherman, S. L. A review of translational animal models for knee osteoarthritis. *Arthritis* **2012**, *2012*, No. 764621.
(16) McCoy, A. M. Animal Models of Osteoarthritis: Comparisons and Key Considerations. *Vet. Pathol.* **2015**, *52*, 803−818.
(17) Kuyinu, E. L.; Narayanan, G.; Nair, L. S.; Laurencin, C. T. Animal models of osteoarthritis: classification, update, and measurement of outcomes. *J. Orthop. Surg. Res.* **2016**, *11*, No. 1165.
(18) Cook, J. L.; Hung, C. T.; Kuroki, K.; Stoker, A. M.; Cook, C. R.; Pfeiffer, F. M.; Sherman, S. L.; Stannard, J. P. Animal models of cartilage repair. *Bone Joint Res.* **2014**, *3*, 89−94.
(19) Teeple, E.; Jay, G. D.; Elsaid, K. A.; Fleming, B. C. Animal models of osteoarthritis: challenges of model selection and analysis. *AAPS J.* **2013**, *15*, 438−446.
(20) Hargrave-Thomas, E. J.; Thambyah, A.; McGlashan, S. R.; Broom, N. D. The bovine patella as a model of early osteoarthritis. *J. Anat.* **2013**, *223*, 651−664.
(21) Pedersen, D. R.; Goetz, J. E.; Kurriger, G. L.; Martin, J. A. Comparative digital cartilage histology for human and common osteoarthritis models. *Orthop. Res. Rev.* **2013**, *2013*, 13−20.
(22) Proffen, B. L.; McElfresh, M.; Fleming, B. C.; Murray, M. M. A comparative anatomical study of the human knee and six animal species. *Knee* **2012**, *19*, 493−499.
(23) Arzi, B.; Wisner, E. R.; Huey, D. J.; Kass, P. H.; Hu, J.; Athanasiou, K. A. A proposed model of naturally occurring osteoarthritis in the domestic rabbit. *Lab Anim.* **2012**, *41*, 20−25.
(24) Poole, R.; Blake, S.; Buschmann, M.; Goldring, S.; Laverty, S.; Lockwood, S.; Matyas, J.; McDougall, J.; Pritzker, K.; Rudolphi, K.; van den Berg, W.; Yaksh, T. Recommendations for the use of preclinical models in the study and treatment of osteoarthritis. *Osteoarthritis Cartilage* **2010**, *18*, S10−S16.
(25) Ferdowsian, H. R.; Durham, D. L.; Kimwele, C.; Kranendonk, G.; Otali, E.; Akugizibwe, T.; Mulcahy, J. B.; Ajarova, L.; Johnson, C. M. Signs of mood and anxiety disorders in chimpanzees. *PLoS One* **2011**, *6*, No. e19855.
(26) Loeser, R. F. Integrin-mediated attachment of articular chondrocytes to extracellular matrix proteins. *Arthritis Rheum.* **1993**, *36*, 1103−1110.
(27) Mayne, R.; Vail, M. S.; Mayne, P. M.; Miller, E. J. Changes in type of collagen synthesized as clones of chick chondrocytes grow and eventually lose division capacity. *Proc. Natl. Acad. Sci. U.S.A.* **1976**, *73*, 1674−1678.
(28) Benya, P. D.; Shaffer, J. D. Dedifferentiated chondrocytes reexpress the differentiated collagen phenotype when cultured in agarose gels. *Cell* **1982**, *30*, 215−224.
(29) Grimshaw, M. J.; Mason, R. M. Bovine articular chondrocyte function in vitro depends upon oxygen tension. *Osteoarthritis Cartilage* **2000**, *8*, 386−392.
(30) Glowacki, J.; Trepman, E.; Folkman, J. Cell shape and phenotypic expression in chondrocytes. *Proc. Soc. Exp. Biol. Med.* **1983**, *172*, 93−98.
(31) Darling, E. M.; Pritchett, P. E.; Evans, B. A.; Superfine, R.; Zauscher, S.; Guilak, F. Mechanical properties and gene expression of chondrocytes on micropatterned substrates following dedifferentiation in monolayer. *Cell. Mol. Bioeng.* **2009**, *2*, 395−404.
(32) Pauly, H. M.; Place, L. W.; Haut Donahue, T. L.; Kipper, M. J. Mechanical Properties and Cell Compatibility of Agarose Hydrogels Containing Proteoglycan Mimetic Graft Copolymers. *Biomacromolecules* **2017**, *18*, 2220−2229.
(33) Jiang, S.; Liu, S.; Feng, W. PVA hydrogel properties for biomedical application. *J. Mech. Behav. Biomed. Mater.* **2011**, *4*, 1228−1233.
(34) Destaye, A. G.; Lin, C. K.; Lee, C. K. Glutaraldehyde vapor cross-linked nanofibrous PVA mat with in situ formed silver nanoparticles. *ACS Appl. Mater. Interfaces* **2013**, *5*, 4745−4752.
(35) Mishra, S.; Ahrenkiel, S. P. Synthesis and Characterization of Electrospun Nanocomposite TiO2 Nanofibers with Ag Nanoparticles for Photocatalysis Applications. *J. Nanomater.* **2012**, *2012*, No. 902491.
(36) Whitesides, G. M.; Ostuni, E.; Takayama, S.; Jiang, X.; Ingber, D. E. Soft Lithography in Biology and Biochemistry. *Annu. Rev. Biomed. Eng.* **2001**, *3*, 335−373.
(37) Kim, L.; Toh, Y. C.; Voldman, J.; Yu, H. A practical guide to microfluidic perfusion culture of adherent mammalian cells. *Lab Chip* **2007**, *7*, 681−694.
(38) Wood, S. T.; Long, D. L.; Reisz, J. A.; Yammani, R. R.; Burke, E. A.; Klomsiri, C.; Poole, L. B.; Furdui, C. M.; Loeser, R. F. Cysteine-Mediated Redox Regulation of Cell Signaling in Chondrocytes Stimulated With Fibronectin Fragments. *Arthritis Rheumatol.* **2016**, *68*, 117−1126.
(39) Buschmann, M. D.; Gluzband, Y. A.; Grodzinsky, A. J.; Kimura, J. H.; Hunziker, E. B. Chondrocytes in agarose culture synthesize a mechanically functional extracellular matrix. *J. Orthop. Res.* **1992**, *10*, 745−758.
(40) Hutter, J. L.; Bechhoefer, J. Calibration of atomic-force microscope tips. *Rev. Sci. Instrum.* **1993**, *64*, 1868−1873.
(41) Walters, D. A.; Cleveland, J. P.; Thomson, N. H.; Hansma, P. K.; Wendman, M. A.; Gurley, G.; Elings, V. Short cantilevers for atomic force microscopy. *Rev. Sci. Instrum.* **1996**, *67*, 3583−3590.
(42) Darling, E. M.; Zauscher, S.; Guilak, F. Viscoelastic properties of zonal articular chondrocytes measured by atomic force microscopy. *Osteoarthritis Cartilage* **2006**, *14*, 571−579.
(43) Salerno, M.; Dante, S.; Patra, N.; Diaspro, A. AFM measurement of the stiffness of layers of agarose gel patterned with polylysine. *Microsc. Res. Tech.* **2010**, *73*, 982−990.
(44) Darling, E. M.; Wilusz, R. E.; Bolognesi, M. P.; Zauscher, S.; Guilak, F. Spatial mapping of the biomechanical properties of the pericellular matrix of articular cartilage measured in situ via atomic force microscopy. *Biophys. J.* **2010**, *98*, 2848−2856.
(45) Ghetie, V.; Schell, H. D. Drying of agarose gel beads. *Experientia* **1971**, *27*, 1384−1385.
(46) Ahmed, E. M. Hydrogel: Preparation, characterization, and applications: A review. *J. Adv. Res.* **2015**, *6*, 105−121.

https://dx.doi.org/10.1021/acsami.9b22596
ACS Appl. Mater. Interfaces 2020, 12, 14814−14824

(47) Hassan, C. M.; Peppas, N. A. Structure and Morphology of Freeze/Thawed PVA Hydrogels. *Macromolecules* **2000**, *33*, 2472−2479.
(48) Kudo, K.; Ishida, J.; Syuu, G.; Sekine, Y.; Ikeda-Fukazawa, T. Structural changes of water in poly(vinyl alcohol) hydrogel during dehydration. *J. Chem. Phys.* **2014**, *140*, No. 044909.
(49) Hynd, M. R.; Frampton, J. P.; Dowell-Mesfin, N.; Turner, J. N.; Shain, W. Directed cell growth on protein-functionalized hydrogel surfaces. *J. Neurosci. Methods* **2007**, *162*, 255−263.
(50) Darling, E. M.; Pritchett, P. E.; Evans, B. A.; Superfine, R.; Zauscher, S.; Guilak, F. Mechanical properties and gene expression of chondrocytes on micropatterned substrates following dedifferentiation in monolayer. *Cell. Mol. Bioeng.* **2009**, *2*, 395−404.
(51) Zhou, M.; Yuan, X.; Yin, H.; Gough, J. E. Restoration of chondrocytic phenotype on a two-dimensional micropatterned surface. *Biointerphases* **2015**, *10*, No. 011003.
(52) Fang, Y.; Eglen, R. M. Three-Dimensional Cell Cultures in Drug Discovery and Development. *SLAS Discovery* **2017**, *22*, 456−472.
(53) Rosenzweig, D. H.; Matmati, M.; Khayat, G.; Chaudhry, S.; Hinz, B.; Quinn, T. M. Culture of primary bovine chondrocytes on a continuously expanding surface inhibits dedifferentiation. *Tissue Eng., Part A* **2012**, *18*, 2466−2476.
(54) Surrao, D. C.; Khan, A. A.; McGregor, A. J.; Amsden, B. G.; Waldman, S. D. Can microcarrier-expanded chondrocytes synthesize cartilaginous tissue in vitro? *Tissue Eng., Part A* **2011**, *17*, 1959−1967.
(55) Hu, X.; Li, D.; Gao, C. Chemically cross-linked chitosan hydrogel loaded with gelatin for chondrocyte encapsulation. *Biotechnol. J.* **2011**, *6*, 1388−1396.
(56) Duarte Campos, D. F.; Drescher, W.; Rath, B.; Tingart, M.; Fischer, H. Supporting Biomaterials for Articular Cartilage Repair. *Cartilage* **2012**, *3*, 205−221.
(57) O'Connell, G. D.; Lima, E. G.; Bian, L.; Chahine, N. O.; Albro, M. B.; Cook, J. L.; Ateshian, G. A.; Hung, C. T. Toward engineering a biological joint replacement. *J Knee Surg.* **2012**, *25*, 187−196.
(58) DuRaine, G. D.; Brown, W. E.; Hu, J. C.; Athanasiou, K. A. Emergence of scaffold-free approaches for tissue engineering musculoskeletal cartilages. *Ann. Biomed. Eng.* **2015**, *43*, 543−554.
(59) Lee, J. K.; Responte, D. J.; Cissell, D. D.; Hu, J. C.; Nolta, J. A.; Athanasiou, K. A. Clinical translation of stem cells: insight for cartilage therapies. *Crit. Rev. Biotechnol.* **2014**, *34*, 89−100.
(60) Cooke, M. E.; Pearson, M. J.; Moakes, R. J. A.; Weston, C. J.; Davis, E. T.; Jones, S. W.; Grover, L. M. Geometric confinement is required for recovery and maintenance of chondrocyte phenotype in alginate. *APL Bioeng.* **2017**, *1*, No. 016104.
(61) Priest, D. G.; Tanaka, N.; Tanaka, Y.; Taniguchi, Y. Micropatterned agarose gel devices for single-cell high-throughput microscopy of *E. coli* cells. *Sci. Rep.* **2017**, *7*, No. 17750.
(62) Tsai, W. B.; Chen, W. T.; Chien, H. W.; Kuo, W. H.; Wang, M. J. Poly(dopamine) coating of scaffolds for articular cartilage tissue engineering. *Acta Biomater.* **2011**, *7*, 4187−4194.
(63) Han, L.; Wang, M.; Li, P.; Gan, D.; Yan, L.; Xu, J.; Wang, K.; Fang, L.; Chan, C. W.; Zhang, H.; Yuan, H.; Lu, X. Mussel-Inspired Tissue-Adhesive Hydrogel Based on the Polydopamine-Chondroitin Sulfate Complex for Growth-Factor-Free Cartilage Regeneration. *ACS Appl. Mater. Interfaces* **2018**, *10*, 28015−28026.
(64) Ball, V. Polydopamine Nanomaterials: Recent Advances in Synthesis Methods and Applications. *Front. Bioeng. Biotechnol.* **2018**, *6*, No. 109.
(65) Yu, Q.-H.; Zhang, C.-M.; Jiang, Z.-W.; Qin, S.-Y.; Zhang, A.-Q. Mussel-Inspired Adhesive Polydopamine-Functionalized Hyaluronic Acid Hydrogel with Potential Bacterial Inhibition. *Global Challenges* **2020**, *4*, No. 1900068.
(66) Harvey, S.; Ng, D. Y. W.; Szelwicka, J.; Hueske, L.; Veith, L.; Raabe, M.; Lieberwirth, I.; Fytas, G.; Wunderlich, K.; Weil, T. Facile synthesis of ultrasmall polydopamine-polyethylene glycol nanoparticles for cellular delivery. *Biointerphases* **2018**, *13*, No. 06D407.

https://dx.doi.org/10.1021/acsami.9b22596
ACS Appl. Mater. Interfaces 2020, 12, 14814−14824